



## Judicious choice of the building compactness to improve thermo-aeraulic comfort in hot climate

S.M.A. Bekkouche<sup>a,\*</sup>, T. Benouaz<sup>b</sup>, M. Hamdani<sup>a</sup>, M.K. Cherier<sup>a</sup>, M.R. Yaiche<sup>c</sup>, N. Benamrane<sup>a</sup>

<sup>a</sup> Unité de Recherche Appliquée en Energies Renouvelables, URAER, Centre de Développement des Energies Renouvelables, CDER, 47133, Ghardaïa, Algeria

<sup>b</sup> University of Tlemcen, BP. 119, Tlemcen R.p. 13000, Algeria

<sup>c</sup> Centre de Développement des Energies Renouvelables, CDER, BP 62 Route de l'Observatoire, Bouzaréah, 16340, Algiers, Algeria

### ARTICLE INFO

#### Article history:

Received 30 November 2014

Received in revised form

4 March 2015

Accepted 12 March 2015

Available online 16 March 2015

#### Keywords:

Multi-zone model

Nodal method

Temperature

Specific humidity

Form factor

Compactness index

Wall sizes

### ABSTRACT

The geometric shape and arrangement of the buildings have a great influence on the indoor climate. Compactness is one of the most important factors, which reduces heating and cooling requirements. These parameters result from geometrical concepts, used to maximize the internal volume of the structure according to its shape. The present study aims at developing a new approach for transient thermal behavior simulation of multizone buildings in Saharan climate. Thermal nodal method was used to apprehend thermo-aeraulic behavior of air subjected to varied solicitations.

As result, this work proves that the compactness is better when the compactness index is lower. For this reason, we must privilege some urban typologies such as the rows of terraced houses, collective buildings and high-dimensional buildings.

© 2015 Elsevier Ltd. All rights reserved.

### 1. Introduction

In desert regions, poor adaptation of the building design and its indoor environment can result in a greater need for active climatisation and, thus, increased energy use. In a warm and dry climate, the design and construction of a building involve the adoption of three elements: typology, shape and technology. The shape of a building is one of the keys to achieving the relationship between cost and performance. A building is an inhabitable volume delineated by an enveloping surface that separates it from the exterior. The relationship between this surface and the volume contained is usually called the shape factor or the compactness index of a building. This coefficient is responsible for the characterization of the contact mode of the building with the exterior [1–2], and it is considered only from the point of view of compactness. Thermal behavior analysis is very important both for the control of indoor comfort conditions and energy requirements. However, the relationship between shape and energy requirements is still an open question [3].

In the professional practice, the most used index is the shape coefficient defined as the ratio between the envelope surface of

the building (i.e. the external skin surfaces) and the inner volume of the building [3]. In this field, several studies have been made. Depecker et al. [4] studied the relationship between shape and energy requirements during the winter season in two French localities with different climate conditions. In Ref. [5], energy consumption was analyzed according to building shape and mixed-use development through quantitative data and a review of the energy consumption characteristics of the residents through empirical surveys. Tsanasa and Xifarab [6] conducted a study on the effect of the relative compactness and other input variables on heating load and cooling load of residential buildings. Granadeiro et al. [7] mention that the architectural design variables which most influence the energy performance of a building are the envelope materials, shape and window areas. Designers require simple tools to obtain information about the energy performance of the building. The shape factor is one of those tools. However, in Ref. [8], it is noted that shape coefficient is a key factor to evaluate building energy efficiency. Heat transfer quantity through envelope is obviously different due to different building shapes. Aksoy and Inalli [9] also studied the building orientation and shape as practical passive parameters. They demonstrated the importance of building orientation and shape to extract solar energy effectively. Therefore, several elements, such as southern window and northern façade insulation, natural ventilation, zoning plan elements, should be considered and determined during the

\* Correspondence to: URAER & B.P. 88, ZI, Gart Taam, Ghardaïa 47000, Algeria. Fax: +213 29 87 01 52.

E-mail address: [smabekkouche@yahoo.fr](mailto:smabekkouche@yahoo.fr) (S.M.A. Bekkouche).

## Nomenclature

$S$	surface ( $m^2$ )		conditioning (W)
$j$	number of the inner surface (wall, door and window) in zone $i$	$V(i)$	volume of zone $i$
$NW(i)$	total number of the interior surfaces (wall, door and window) in zone $i$	$v_s(i)$	specific volume of the humid air in the zone $i$
$T_{ai}(n)$	air temperature of the zone $n$ =air température entering the zone $i$ (K)	$e$	thickness (m)
$T_{sij}, T_A$	temperature of surface $j$ in zone $i$ (K)	$n$	number of node
$r_s(i)$	specific humidity: mass of water vapor contained in the unit mass of dry air ( $kg_{vap}/kg_{as}$ or %)	$\alpha$	absorption coefficient
$H_r$	relative humidity (%)	$\varepsilon$	thermal emissivity
$P_{sat}$	pressure of saturation vapor (Pa)	$G$	the incident global irradiation on the surfaces ( $W m^{-2}$ )
$L_v$	latent heat of vaporization of water ( $J kg^{-1}$ )	$\lambda$	thermal conductivity ( $W K^{-1} m^{-1}$ )
$C_v$	heat capacity at constant volume ( $J kg^{-1} K^{-1}$ )	$c_p$	specific heat ( $J kg^{-1} K^{-1}$ )
$C_{as}$	heat capacity of the air mass ( $J kg^{-1} K^{-1}$ )	$\rho$	density ( $kg m^{-3}$ )
$H_s, H_L$	sensitive and latent enthalpy of the humid air (J)	$F$	form factor between the exchange surfaces
$H^e(i)$	enthalpy of the humid air mass entering the zone $i$ (J)	$\sigma$	Stefan–Boltzmann constant ( $W m^{-2} K^{-4}$ )
$H^{leav}(i)$	enthalpy of the humid air mass leaving the zone $i$ (J)	$V_{vent}$	wind speed ( $m s^{-1}$ )
$Q_{mas}^{trans}(n, i)$	mass flow transiting from zone $n$ to zone $i$ (kg/s)	$h_{conv}$	convective transfer coefficients ( $W m^{-2} K^{-1}$ )
$Q_{mas}^{trans}(i, n)$	mass flow of the dry air transiting from zone $i$ to zone $n$ (kg/s)	$M_{as}$	molar mass of dry air ( $g mol^{-1}$ )
$Cl_s, Cl_L$	internal sensitive and latent powers due to appliances, occupants, lighting...(W)	$M_v$	molar mass of water vapor ( $g mol^{-1}$ )
$P_s, P_L$	sensitive and latent powers provided by the air-	$P$	total pressure (Pa)
		$P_{vs}$	saturated vapor pressure (Pa)
		$Gr$	Grashof number
		$Pr$	Prandtl number
		$h_{conv}$	the heat exchange coefficient by convection ( $W/m^2 K$ )
		$\Delta T$	temperature difference between the wall and the surrounding air (K)
		$L$	characteristic length (m)

schematic design phase. As these kinds of elements strongly influence building shape and size, they are directly related to construction costs as well as energy performance [10]. In [11] it is proved that generally, annual energy consumption increases as the courtyard building shape gets longer as a direction of prevailing wind.

A simplified thermal model for the prediction of the thermal performance of buildings is proposed by Mathews et al. [12]. In [13] a coupling between a building thermal simulation code and genetic algorithm was made to estimate the internal temperatures. However, the effect of the choice of thermal comfort model on the building's energy use is analyzed by Sourbron and Helson [14]. While Siddharth et al. [15] mentioned in their article that there are a limited number of available techniques for non-linear systems.

In these works, a method for reducing the order of dynamic models of temperature and humidity in multi-zone buildings is proposed. With the present studies, we can aim the advantage of a proposed new approach to the description of the thermo-aeraulic behavior in a multizone building. The evaluation is derived from a series of computer simulations. The most of current building simulation programs lack the capability to properly model emerging building energy systems due to the negligence of the humidity. Thermo-aeraulic modeling is essential for establishing overall thermal performance values and understand how different assembly designs perform under different interior and exterior climate conditions. This tool is used to evaluate the performance of a proposed architecture for a real building located in a very hot climate. We propose from a geometric analysis, an evaluation of the temperature and the specific humidity according the contact mode, geometric form, and making enlargement plans. Through the expected results, we can address a significant technical guide to the architect. Our contribution essentially allows us to offer the best technical solutions in terms of: dimensions intended to be used in the design of buildings, preferred building size and the most recommended geometric form for the realization of such building components.

## 2. Multizone building modeling

Developing a detailed thermal building simulation model may take several months if not a year of development time. Commercially available detailed building energy simulation programs, such as EnergyPlus [16], TRNSYS [17], and DOE-2 [18]. These software are powerful tools allow to introduce the input parameters to obtain output parameters without properly understanding the physical mechanisms of heat and mass transfer inside the habitat. It is in this context that we are obliged to program and understand in detail all existing phenomena in the solar system.

To determine the thermal comfort level in a thermal environment implies analyzing a complex interaction of many variables. Thus it is essential to constantly ensure the following parameters of thermal comfort:

- Ambient indoor temperature.
- The mean radiation temperature: this temperature is affected by all direct or indirect radiation that impinges onto the individual. In our case, we consider that the building is uninhabited. However, an acceptable approximation can be made by regarding only the thermal radiation given off by the walls [19]. This parameter depends on both the surface temperature and the surface area of walls. Our model can deliver these temperatures without any problems.
- Air velocity: it is directly related to the mass flow, therefore, it is considered in the proposed mathematical model.
- Specific or relative humidity, they are related by the Eq. (24) and are also taken into consideration.

One of the fundamental laws of physics states that mass can neither be produced nor destroyed, i.e. mass is conserved. Although energy can change in form, it can not be created or destroyed. These two laws of physics provide the basis for two tools which are used routinely in environmental engineering and science “the mass balance and the enthalpy balance”, knowing that

the enthalpy is a measure of the total energy of a thermodynamic system.

### 2.1. Enthalpy balance

Assuming that an area “zone  $i$ ” is in contact with  $N+1$  other zone, outside is represented by area  $N^{\circ} 0$ . For the zone  $i$ , the enthalpy change per unit time is written by the following equation [20]:

$$\frac{dH(i)}{dt} = \frac{dH^e(i)}{dt} - \frac{dH^{leav}(i)}{dt} + \sum_{j=i}^{NW(i)} S_j h_{cij} (T_{sij}(i) - T_{al}(i)) + P_L + P_S + Cl_L + Cl_S \quad (1)$$

with

$$H^e(i) = \sum_{n=0}^N Q_{mas}^{trans}(n, i) (T_{al}(n) C_{as} + r_s(n)) (L_v + C_v T_{al}(n)) \quad (2)$$

$$H^{leav}(i) = \sum_{n=0}^N Q_{mas}^{trans}(i, n) (T_{al}(i) C_{as} + r_s(i)) (L_v + C_v T_{al}(i)) \quad (3)$$

$\sum_{j=i}^{NW(i)} S_j h_{cij} (T_{sij}(i) - T_{al}(i))$ : expressions of the convective flow exchange between surfaces  $j$  of walls for zone  $i$  corresponding to a temperature  $T_{sij}$  and the air mass in this zone corresponding to a temperature  $T_{al}$  (W).

Expression of convective transfer coefficients due to exchange between the air and walls inner surfaces is given in Table 1:

### 2.2. Mass balance of dry air

In the building thermal, temporal variations in mass are very low amounts, which allow simplification of the conservation equation of air mass in zone  $i$  [20].

$$\begin{aligned} & \sum_{n=0}^N Q_{mas}^{trans}(n, i) - Q_{mas}^{trans}(i, n) \\ &= \frac{dm_{as}}{dt} \\ &\approx 0 \\ &\Rightarrow \sum_{n=0}^N Q_{mas}^{trans}(n, i) \\ &= \sum_{n=0}^N Q_{mas}^{trans}(i, n) \end{aligned} \quad (4)$$

This equation reflects that the sum of the mass flows of dry air entering the zone  $i$  is equal to the sum of the mass flows leaving

the zone  $i$ . This equation allows us, hereinafter, to simplify the writing of enthalpy balances.

### 2.3. Enthalpy changes: sensible and latent balance

An enthalpy change describes the change in enthalpy observed in the constituents of a thermodynamic system when undergoing a transformation or chemical reaction [20].

$$H(i) = H_s(i) + H_L(i) = m_{as} C_{as} T_{al}(i) + m_{as} r_s(i) (L_v + C_v T_{al}(i)) \quad (5)$$

We can neglect  $m_{as} C_v T_{al}(i)$  if we compare this amount with  $m_{as} r_s(i) L_v$ ,  $L_v = 2500$  kJ/kg and  $C_v = 1.96$  kJ/kgK. Therefore,

$$H_s(i) \approx m_{as} C_{as} T_{al}(i) \quad (6)$$

$$H_L(i) \approx m_{as} r_s(i) L_v \quad (7)$$

This helps to write the following equation:

$$\frac{dH(i)}{dt} = \frac{dH_s^e(i)}{dt} - \frac{dH_s^{leav}(i)}{dt} \quad (8)$$

This simplification allows us to write two equations of enthalpy balance [20]:

- Sensible balance: as a function only of  $T_{al}$ .
- Latent balance: as a function only of  $r_s$ .

#### 2.3.1. Sensible balance

As we have already mentioned, in the building thermal, temporal variations in mass are very low amounts, the change in enthalpy can be assimilated to the variation in temperature:

$$\frac{dH_s(i)}{dt} = \frac{d(m_{as} C_{as} T_{al}(i))}{dt} = C_{as} \frac{dm_{as}}{dt} T_{al}(i) + C_{as} \frac{dT_{al}(i)}{dt} m_{as} \quad (9)$$

$$\begin{aligned} \frac{dH_s(i)}{dt} &= \frac{dH_s^e(i)}{dt} - \frac{dH_s^{leav}(i)}{dt} + \sum_{j=i}^{NW(i)} S_j h_{cij} (T_{sij}(i) - T_{al}(i)) + P_S \\ &+ Cl_S \end{aligned} \quad (10)$$

From this result, the following equation was obtained for the temperature function:

$$\begin{aligned} \rho_{as} C_{as} V(i) \frac{dT_{al}(i)}{dt} &= \sum_{i=0}^N [Q_{mas}^{trans}(i, n) C_{as} (T_{al}(n) - T_{al}(i))] \\ &+ \sum_{j=i}^{NW(i)} [S_j h_{cij} (T_{sij}(i) - T_{al}(i))] + P_S + Cl_S \end{aligned} \quad (11)$$

We obtain a system of  $N$  equations with  $N$  unknowns; the main variables are the air temperatures in each zone. The surface temperature  $T_{sij}$  will be obtained by establishing thermal balance of the wall inner surface. It is through these balances that we see couplings with other modes of heat transfer [20].

#### 2.3.2. Latent balance

In the same manner as the sensible balance, neglecting the term  $dm_{as}/dt$ , and with using the simplified conservation equation of the dry air mass, we get the equation 15 [20]:

$$\frac{H_L(i)}{dt} = \frac{dH_L^e(i)}{dt} - \frac{dH_L^{leav}(i)}{dt} + P_L + Cl_L \quad (12)$$

$$m_{as}(i) = \frac{V(i)}{v_s(i)} \quad (13)$$

**Table 1**  
Expression of convective transfer coefficients [21].

Surface description	Flow regime	Condition	Expression
Vertical wall	Laminar regime	$10^4 < Gr$ $Pr < 10^9$	$h_{Conv} = 1.42 (\Delta T/L)^{1/4}$
	Turbulent regime	$Gr Pr > 10^9$	$h_{Conv} = 1.31 (\Delta T/L)^{1/3}$
An upper surface of a hot horizontal plate or an underside surface of a cold plate	Laminar regime	$10^4 < Gr Pr$ $< 10^9$	$h_{Conv} = 1.32 (\Delta T/L)^{1/4}$
	Turbulent regime	$Gr Pr > 10^9$	$h_{Conv} = 1.52 (\Delta T/L)^{1/3}$
An underside surface of a hot plate or an upper surface of a cold plate	Laminar regime	$10^4 < Gr Pr$ $< 10^9$	$h_{Conv} = 0.59 (\Delta T/L)^{1/4}$
	Turbulent regime	$Gr Pr > 10^9$	

$$\frac{dH_L(i)}{dt} = \frac{d(m_{as}r_s(i)Lv)}{dt} = Lv\frac{dm_{as}}{dt}r_s(i) + Lv\frac{dr_s(i)}{dt}m_{as} \quad (14)$$

$$m_{as}(i)\frac{dr_s(i)}{dt} = \sum_{i=0}^N [Q_{mas}^{trans}(i, n)(r_s(n)-r_s(i))] + \frac{P_L}{L_v} + \frac{C_{L_L}}{L_v} \quad (15)$$

As for the sensitive balance, a system of  $N$  equations with  $N$  unknowns is obtained; the main variables are the specific humidities in each zone.

We can use the empirical formulas of Nadeau and Puiggali [22]; specific humidity may be expressed as a function of relative humidity by the relationship:

$$H_s = \frac{0.622P_{sat}(T)Hr}{101325 - P_{sat}(T)Hr} \quad (16)$$

$$P_{sat}(T) = e^{23.3265 - \frac{3802.7}{T} - \left[\frac{472.68}{T}\right]^2} \quad (17)$$

In this contribution, thermal nodal method was used to apprehend temperature and specific humidity of air subjected to varied solicitations. The nodal analysis is a powerful method; it has been used in several branches such as solar energy systems [23], micro-electronics [24] or also the spatial field [25]. We will gradually use this approach in the domain of building's physics and we will interest ourselves in the automatic generation of nodal models. The building energy balance for a zone is a balance model with one air node per zone, representing the temperature and the specific humidity of the zone air volume.

#### 2.4. Conduction model and superficial exchanges

For coupling superficial exchanges and to calculate the conduction heat transfer, we can base on the conduction model given in [2,26–31]. In this paper, the proposed approach allows representing the multilayer system by a model based on an electrical analogy proposed by Rumianowski et al. in 1989, and then it was taken by Con et al. in 2003 [32]. It is often used when we interest to the determination of the temperature of any node inside a wall. For an envelope's wall, we suppose that we have two temperatures as conditions to a surface's limits. In the hypothesis of mono-dimensional conductive transfers, the study's frame is then divided into a determined number of elements supposed in each moment of a uniform temperature. The transposition of the thermal problem of conduction into an electrical problem is called thermo-electrical analogy. This reasoning is explained in detail in previous works [2]. The nodes, which in an electrical meaning symbolize equipotentials, correspond to isotherm lines. Applied to the mono-dimensional conduction in a wall, those isothermal elements are isothermal slices sprung from our discretization hypothesis. Then, those nodes are linked to each other by the analogical resistance of the physical layer of the wall which divides them. Therefore, each of those nodes is getting an electrical capacitor, traducing the thermal storage of the corresponding wall's part, and allowing in this the traduction of the thermal inertia effects [2]. The energy balance of the building for surfaces is represented in [2–33].

#### 2.5. Calculation of the form factor

The variation in the geometric shape of the building causes a modification of the surface exchange with indoor air (heat exchange by convection) and with other surfaces surrounding the same area (radiation heat exchange). This latter mode depends on exchange surfaces of the various opaque walls, walls temperatures and the form factor between receiving and emissive surface. From this factor, we

can describe the arrangement of a surface relative to the other surface. Therefore, the variation in wall surface evokes a radical change in this factor which is purely geometric. Indeed, the evaluation of form factor is numerically complex and computationally demanding. Researchers prefer to use nomograms when they exist, instead of seeking analytical solutions. In this contribution, we will use the analytical solutions which have many advantages in particular accuracy. In summary, we can conclude that when changing walls properties, automatically there will be radical changes in sensible and latent balance since the heat flux exchanged by conduction, convection and radiation will also be changed.

First, we are interested in calculating the form factor between two plane-parallel rectangular surfaces, of any dimensions, centered or/and not centered. In this regard, it provides a descriptive diagram of the geometric problem in Fig. 1.

Assuming that

$$\begin{aligned} MM' &= r, \\ OO'' &= \rho_0(a_0, b_0, 0), \\ O'M' &= \rho'(X', Y', 0), \\ r^2 &= (X-X'-a_0)^2 + (Y-Y'-b_0)^2 + d^2, \\ O'O' &= d, \\ \cos \theta &= \cos \theta' = d/r \end{aligned}$$

Surfaces dimensions

$$-a(X' + a - b(Y' + b - a'(X' + a' - b'(Y' + b' -$$

The form factor is calculated by solving the following integral [34]:

$$F_{12} = \frac{1}{\pi S'} \int_S \int_{S'} \frac{\cos(\theta) \cos(\theta') ds ds'}{r^2} = \frac{d^2}{\pi S'} \int_S \int_{S'} \frac{ds ds'}{r^4} \quad (18)$$

In order to generalize the results, we introduce the reduced dimensions surfaces that are well noted.

$$X = a/d, Y = b/d, X_0 = a_0/d, X' = a'/d, Y' = b'/d, Y_0 = b_0/d$$

Eq. (1) becomes [34]:

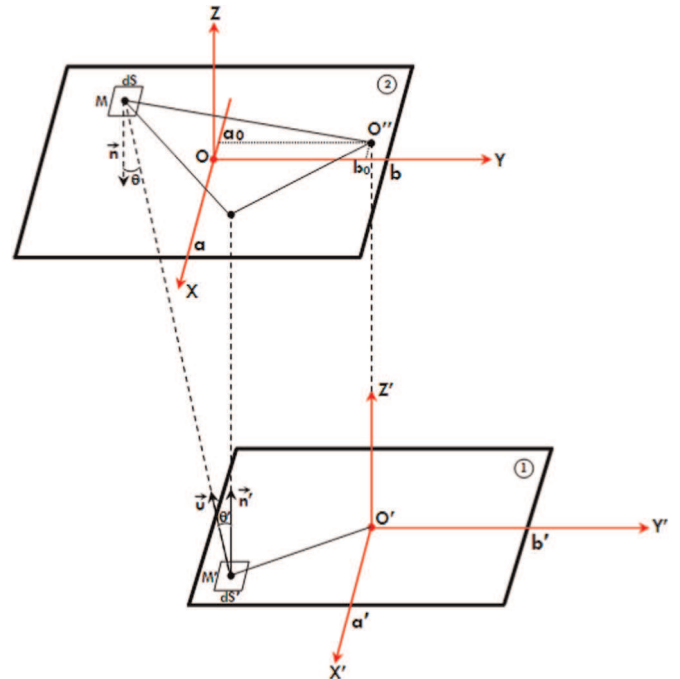


Fig. 1. Descriptive diagram of the geometric problem: plane-parallel rectangular surfaces.

$$F_{12} = \frac{1}{8\pi X'Y'} \left( \begin{array}{c} F(X-X_0+X', Y-Y_0+Y') - F(X-X_0+X', Y-Y_0-Y') + F(X-X_0+X', Y+Y_0-Y') - \\ F(X-X_0+X', Y+Y_0+Y') - F(X-X_0-X', Y-Y_0+Y') + F(X-X_0-X', Y-Y_0-Y') - \\ F(X-X_0-X', Y+Y_0-Y') + F(X-X_0-X', Y+Y_0+Y') + F(X+X_0+X', Y-Y_0+Y') - \\ F(X+X_0+X', Y-Y_0-Y') + F(X+X_0+X', Y+Y_0-Y') - F(X+X_0+X', Y+Y_0+Y') - \\ F(X+X_0-X', Y-Y_0+Y') + F(X+X_0-X', Y-Y_0-Y') - F(X+X_0-X', Y+Y_0-Y') + \\ F(X+X_0-X', Y+Y_0+Y') \end{array} \right) \quad (19)$$

with

$$F(u, v) = u\sqrt{v^2+1} \operatorname{Arctg} \frac{u}{\sqrt{v^2+1}} + v\sqrt{u^2+1} \operatorname{Arctg} \frac{v}{\sqrt{u^2+1}} - \frac{1}{2} \ln(u^2+v^2+1) \quad (20)$$

This complex formula, but easy to program, is of the great importance. It contains all possible cases to calculate form factors of any flats, parallel surfaces, rectangular or square, centered or not.

The second case corresponds to rectangular surfaces forming a dihedral; an implicit scheme is illustrated in Fig. 2. Assuming that

$$MM' = r, \quad OM' = \rho'(X', Y', 0),$$

$$OM = \rho(0, Y, Z),$$

$$\cos \theta' = (Z/r) \quad \cos \theta = X'/r$$

$$r^2 = X'^2 + (Y-Y')^2 + Z^2$$

The form factor is calculated by solving the following integral [34]:

$$F_{12} = \frac{1}{\pi S'} \int_{S'} \int_S \frac{X'Z ds' ds}{r^4} \quad (21)$$

Similarly, we introduce the following reduced coordinates.

$$X = a/b, \quad Z = c/b$$

This leads to the following equation [34]:

$$F_{12} = \frac{1}{4\pi X} (F(X, Z) - F(X, 0) - F(0, Z)) \quad (22)$$

with

$$F(u, v) = -4\sqrt{u^2+v^2} \operatorname{Arctg} \frac{1}{\sqrt{u^2+v^2}} + (u^2+v^2-1) \ln(u^2+v^2+1) - (u^2+v^2) \ln(u^2+v^2) \quad (23)$$

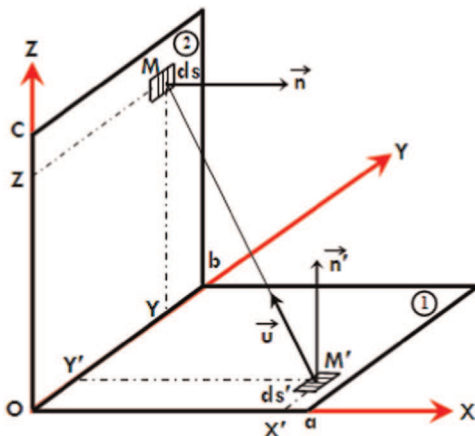


Fig. 2. Descriptive diagram of the geometric problem: plane-parallel rectangular surfaces.

### 3. Description of typical house plan

The study was carried out on a building in Ghardaïa. It is a region whose stones are the most used construction materials. A typical most commonly used construction in the region had been chosen. The house has an area of 149.3450 m<sup>2</sup>; wall heights are equal to 4 m while the other dimensions are shown in detail in Fig. 3 and Table 2.

This apartment includes the following elements:

1. Building envelops consisting of a heavy structure generally constituted of stones (40 cm thick) jointed and surrounded by two layers having thickness of 1.5 cm of mortar cement. The most inner face is coated with 1 cm thick plaster layer.
2. The inner walls (or splitting walls) whose sides are in contact only with the internal ambient are considered to be of heavy structure constructed of stones of 15 cm width jointed and surrounded by two mortar cement layer of 1.5 cm thick and two layers of 1 cm thick of plaster.
3. The flooring is placed on plan ground to lodge the ground floor. The concrete of the flooring is directly poured on the ground thus minimizing losses. Floor tiles are inter-imposed, it is an end coating resisting to corrosion and chemical agents.
4. The roof is composed of cement slabs and concrete slab made so that it handles the load and be economical.
5. Windows and doors contribute significantly to the energetic balance. In this case focus is made particularly on Windows and doors dimensions and all are made of woods. Layer thickness, composition and thermal transmittance values  $U$  for walls, ground and roof are given in Table 2.

Windows shall be designed to limit air leakage. The air infiltration rate shall not exceed 2.8 m<sup>3</sup>/h per linear meter of sash crack when tested under a pressure differential of 75 Pa. We use the  $U$ -value in the first case for glazing. For our study, we consider that the window composition comprises in addition to the configuration given in Table 3, wood blinds usually separated from the previous configuration by an air gap of 2 cm. We assume that the heat transfers through windows are only by conduction. However, the doors are made of wood with a thickness of 2 cm:  $\lambda = 0.14 \text{ W m}^{-1} \text{ K}^{-1}$ ,  $\rho = 500 \text{ kg m}^{-3}$  and  $c_p = 2500 \text{ J kg}^{-1} \text{ K}^{-1}$ ,  $\lambda$ ,  $\rho$  and  $c_p$  are, respectively, thermal conductivity, density and specific heat).

### 4. Climatology of Ghardaïa site and selected data for the simulation

Ghardaïa (32.360 N, 3.810 W and 450 m above MSL) has a hot desert climate, is a dry and arid site, characterized by an exceptional sunshine, most often, it has a very important rate of insolation (75% on average) and the mean annual of global solar radiation measured on horizontal plane exceeds 20 (MJ/m<sup>2</sup>). The

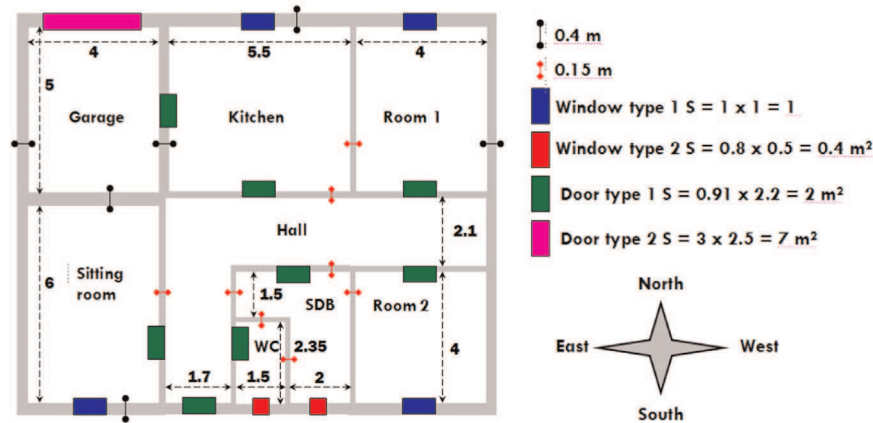


Fig. 3. Descriptive plane: southern orientation, dimensions are given by m.

sunshine duration is more than 3000 h per year, which promotes the use of solar energy in various fields. The maximum temperature in the summer can exceed  $48^\circ\text{C}$  [35].

The climate of the city of Ghardaïa is characterized by low annual precipitation, which is extremely variable. The annual distribution of temperature is fairly uniform. For example, the temperatures of summer vary from  $40^\circ\text{C}$  to  $45^\circ\text{C}$  and the absolute maximum recorded in Ghardaïa is  $47^\circ\text{C}$  in July 2005. Monthly mean amplitudes of temperatures are more moderate in the winter than in the summer (average  $11^\circ\text{C}$  in winter and  $13.5^\circ\text{C}$  in summer). They fluctuate around  $20^\circ\text{C}$ . High values of relative humidity were obtained for low temperatures. Low values of relative humidity were obtained during hot periods. The maximum winds are about  $15 \text{ m/s}$ , occurring during the spring season, and their direction are predominately from north-northeast. Stronger winds in the region of Ghardaïa are mostly prevailing during the period from March to June. On average of 3.3 days of dust storms and 49 blowing sand events occur per year [36].

To perform this study, we chose the days of 23–30 August 2013. The incident solar radiation on a horizontal surface, on a surface tilted at the latitude angle and for a vertical plane facing south, north, east, and west was determined using numerical models [37]. The curve of the incident solar irradiation in Fig. 4 proves that these days correspond to a clear sky, an ambient temperature between 23 and  $43.5^\circ\text{C}$  (Fig. 5) and relative humidity between 17% and 66% (Fig. 6). Fig. 7 shows that the wind velocity undergoes a random behavior, peaks can exceed the value of  $9 \text{ m s}^{-1}$ .

The solar radiation received on a surface depends on the orientation of the surface. A normal surface facing east will receive direct solar radiation at sunrise, while a vertical surface facing west only receives direct radiation after noon (when the sun passes its zenith). A horizontal surface can receive solar radiation during the whole day when no shadowing from the surrounding area appears. As can be seen in Fig. 4, a horizontal surface will receive the most radiation on a sunny day. An east facing (and also a west facing) vertical surface receives more radiation than a south facing vertical surface.

Table 2  
Technical details of the apartment.

Zone	Sitting room	Garage	Kitchen	Room 1	Room 2	SDB	WC	Hall	Habitat
Living space	24	20	27.5	20	16	10.475	3.525	27.8450	149.3450
Total area					181.1700				
Habitable volume	96	80	110	80	64	41.9000	14.1000	111.3800	597.3800
Total volume					797.1480				
Compactness index without exposure of the roof	0.4167	0.4500	0.2000	0.4500	0.5000	0.1909	0.4255	0.1365	0.0373
Compactness index with exposure of the roof	0.6667	0.7000	0.4500	0.7000	0.7500	0.4409	0.6755	0.3865	0.2645

Table 3  
Layer thickness, walls composition and  $U$  values for building envelope.

	Composition	Thickness (cm)	Thermal transmittance values $U$ ( $\text{W m}^{-2} \text{K}^{-1}$ )
Exterior walls	Mortar cement	1.5	1.97
	Stone	40	
	Mortar cement	1.5	
	Coating plaster	1.0	
Interior walls	Mortar cement	1.5	2.82
	Stone	15	
	Mortar cement	1.5	
	Coating plaster	1.0	
Ground	Tiling	2.5	0.93
	Cement	1	
	Stone	6	
	Concrete	24	
Roof	Plaster	1.5	1.05
	Slab	12	
	Mortar	3	
Flat glass	Single pane, clear		5.91

## 5. Numerical simulation and influence of the compactness

In many situations, the practice has shown that the results of the simulations can often accurately reflect actual measurements [38]. Building energy simulation tools are currently widely used to assess the level of comfort in a multizone building [39–42]. The thermo-aeraulic model is based on the nodal method. Studies by this method are very widespread because they require a reduced

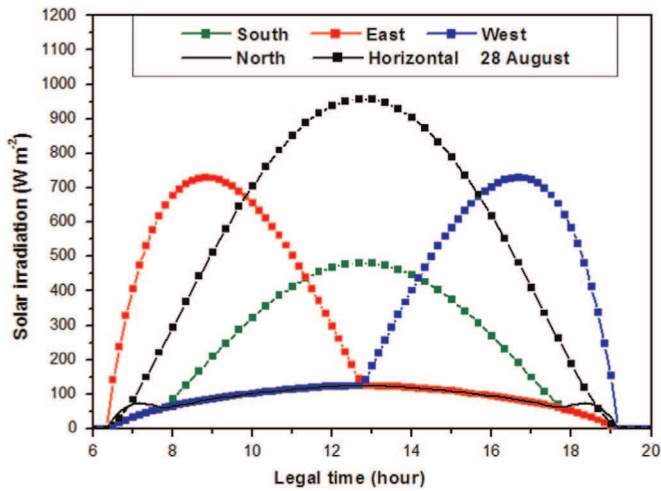


Fig. 4. Incident solar irradiation, 28 August.

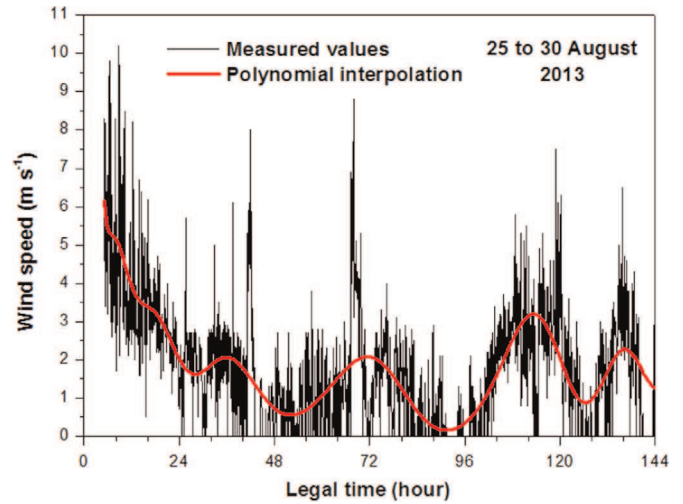


Fig. 7. Wind speed profile, 25–30 August.

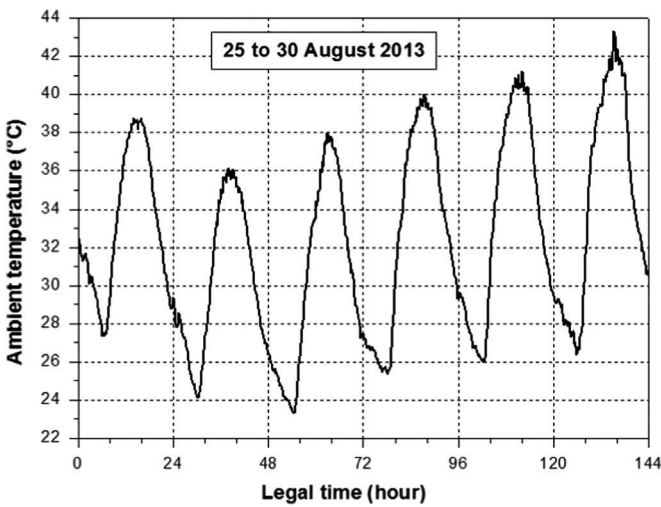


Fig. 5. Ambient temperature profile, 25–30 August.

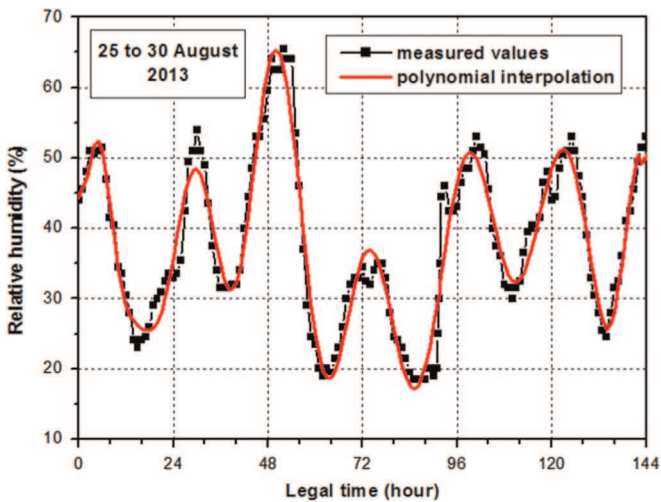


Fig. 6. Variation of the relative humidity, 25–30 August.

formed from electrical analogies. We attribute a type to each node to facilitate the establishment of the mathematical model. The illustration and the role of nodes are explained in detail in reference [2]. To solve the equations system, we used the Runge-Kutta fourth order numerical method. The calculation interval is determined automatically since we use the ode45 command in a program in MATLAB. However, the computing of temperatures and specific humidity is of paramount importance.

First, we will study the influence of the enlargement of an individual building fully exposed to the sun (at the roof and walls). The plan enlargement corresponds to multiplying each surface “S” by the “Agr” expansion parameter, and consequently we multiply the internal volume by “Agr√Agr”. The calculated temperatures of the internal air in room 1 and the kitchen are given below respectively in Figs. 8 and 9 below. The imposed initial conditions are the same for all cases.

Before analyzing the results, it must be taken into account that:

1. The kitchen is more compact than room 1, the compactness index equal to 0.45; it is lower compared to the compactness index of room 1, which equals 0.7.
2. Increasing the size promotes thermal comfort; therefore we must privilege the tall buildings. A very simple example is shown; consider a cube of side length  $L=4$  m, the corresponding index value is 1.25, when we compare to a cube of

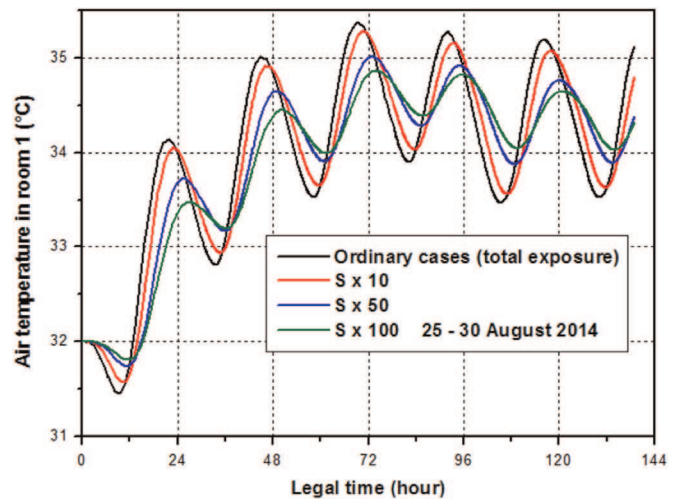


Fig. 8. Simulated temperature of air in room 1, total exposure.

memory capacity and allow having results in a short time. After performing the analysis of the physical phenomena involved in the thermo-aerualic system, we are trying to write a set of algebraic equations. The entire system is divided into a number of elementary volumes supposed isotherms; the resulting equations are

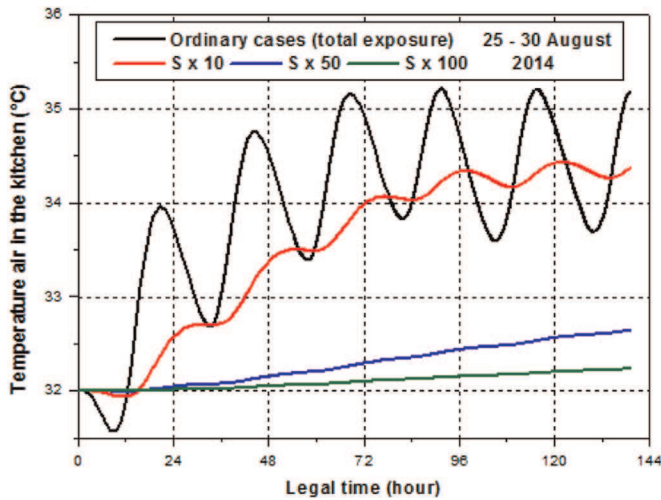


Fig. 9. Simulated temperature of air in the kitchen, total exposure.

side length 8 m, we observe that the compactness index of the new cube is 0.625.

3. The main indicators of thermal comfort are temperature and humidity.

The room air and wall temperatures create the conditions of heat exchange between the human body and the ambiance. We can aggregate these two temperatures into a single parameter; the operative temperature or resulting temperature.

As a first approximation, and for low air speeds, it may be calculated as half the sum of the room air and wall temperatures. In this article, the study is limited to the calculation of the air temperature. However, moisture is the second parameter of comfort; it creates the conditions of heat exchange by cutaneous evaporation. It is usually expressed in relative or specific humidity. Relative humidity expressed as a percentage, is the ratio of the actual partial vapor pressure of water to the saturation vapor pressure at that air temperature.

The comfort range is sufficiently wide, from 30% to 70%. Specific humidity (or moisture content) is the ratio of water vapor mass to the air parcel's total mass and is sometimes referred to as the humidity ratio. Using this definition of relative humidity, the specific humidity can be expressed as [43]

$$r_s = \frac{M_v}{M_{as}} \frac{H_r p_{vs}}{p - H_r p_{vs}} \quad (24)$$

The obtained temperatures for each area prove that the enlargement of this construction improves the level of thermal inertia and provide higher thermal insulation performance. The increasing size consolidates the thermal insulation of the building external envelope and allows maintaining and limiting temperature fluctuations. Thermal insulation can keep an enclosed area such as a building warm, or it can keep the inside of a container cold. Therefore, we can discover the appearance of the high thermal inertia which provides more stable temperature change. We note this aspect in determining the resulting temperature of the room. The air temperature with low compactness (high compactness index) changes significantly during the day, while the temperature of the air with high compactness (low compactness index) does not change as drastically. It can be also characterized by the difference between time of maximum outside air temperature and time of maximum inside air temperature. The maximum temperature of the outside air is about 15 h for the first day. The phase difference is proportional to the compactness and vice versa. When the compactness increases and exceeds a certain

threshold value as the case of the kitchen, and beyond this limit (Sx50 and more), the thermal insulation this time becomes more efficient and provides more lower temperatures.

The second parameter to quantify the air humidity is the specific humidity. It can also be defined according to the parameters of air: the total pressure  $P$  and the partial pressure of water vapor  $P_v$ . In comparison terms, the most favorable value of the specific humidity corresponds to large-scale buildings according to the results shown in Fig. 10. The enlargement of this individual building causes a decrease in specific humidity of indoor air.

In this same reasoning and via Fig. 11, we are also interested in the size influence of a building with double facades in north and south sides. The figure below is an application example destined to determine the air temperature in room 2.

First, it is known that the big advantage of this type of house is the energy economy. Once again, we see that for a similar design, by considering the volume and the wall surfaces as calculation basis, we would tend to advantage the large buildings since the obtained temperatures are closer compared to the thermal comfort temperature. In consequence, energy losses, heating and cooling needs reported to the habitable volume are more important when the dwelling size is smaller. Furthermore, the instantaneous behavior of the specific humidity undergoes almost the same scenario observed in Fig. 11.

Also, the temperatures are lower in this case than for the previous case, thermal insulation is more improved by strengthening the compactness of the building. It helps to maintain better freshness inside the habitat. We then judge that the compactness promotes thermal performance quality insulation.

The evolution curves (Fig. 12) of the compactness factor ( $R$ ) according to the enlargement order and the contact mode show that for a constant shape (the given plane), the compactness is improved proportionally with the building size.

Let us take the third case as indicative example, before reaching a high enlargement level ( $Agr < 10$ ), the slope of trajectory ( $-\Delta R/\Delta Agr$ ) is important, beyond this limit ( $Agr > 10$ ), this variation does not become significant.

Furthermore, as shown in several previous studies, it is known that in terms of comfort, the sphere is the most favorable geometry. This is the form that has less surface contact between the inside and outside. In this context, from a purely geometric analysis, we propose to compare the change in the cell compactness relative to the geometric shape at constant volume. That is to say, by fixing the volume and the  $Agr$  expansion parameter, one can determine the corresponding value of the compactness index. Assuming that  $Agr=1$ , we have the following dimensions:

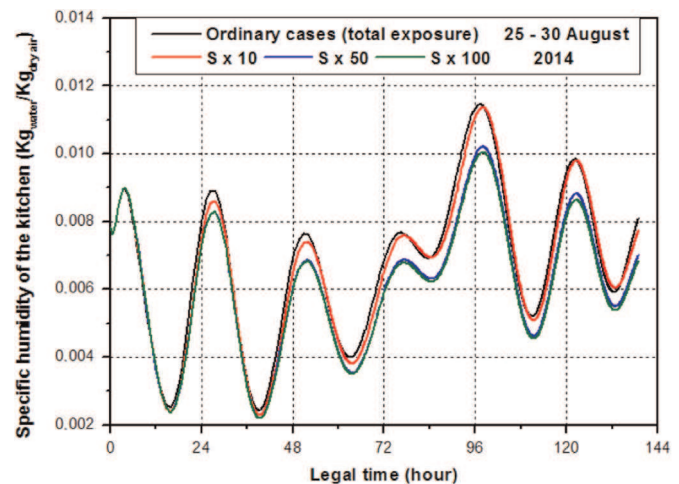


Fig. 10. Simulated specific humidity of air in the kitchen, total exposure.

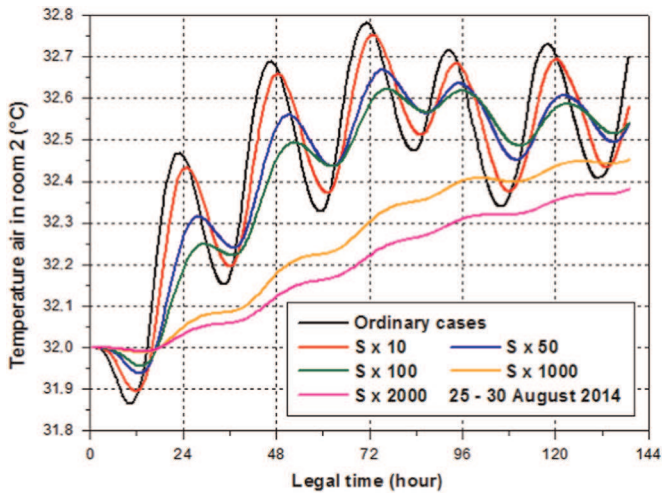


Fig. 11. Simulated temperature of air in room 2.

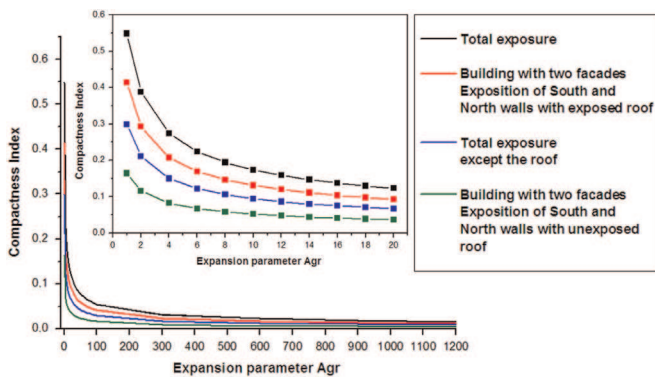


Fig. 12. Variation of the compactness index according to the enlargement order and the contact mode: the plan enlargement corresponds to multiplying each surface by the  $Agr$  expansion parameter and the internal volume by  $Agr\sqrt{Agr}$ .

1.  $V=3.2 \times 10 \times 3$  ( $m^3$ ) for a parallelepipedic form, whose the height is 3 m.
2.  $V=4.5789 \times 4.5789 \times 4.5789$  ( $m^3$ ) for a cubic form

Focusing on the variation of the compactness index of the cell and according to the geometric shape and the  $Agr$  expansion parameter, Fig. 13 depicts three possible cases:

- Case 1: Total exposure.
- Case 2: Building with two facades, Exposition of South and North walls with exposed roof.
- Case 3: Building with two facades, Exposition of South and North walls with unexposed roof.

By combining these results, we prove that the compactness improves with the size because the  $S/V$  ratio decreases and tends to 0 regardless of the geometric form; consequently, the shape influence tends to disappear with increasing size.

For our study, we introduce room 2 as an explicit example for the numerical implementation. Furthermore, to concretely determine the influence of the geometrical shape, we transformed our proposed plan in two different forms such that changing all dimensions (width, length and height) is performed in a uniform way and proportionally with changes in internal dimensions of this room. Geometric shapes (at constant volume) are listed below. These considerations remain true even for doors and windows.

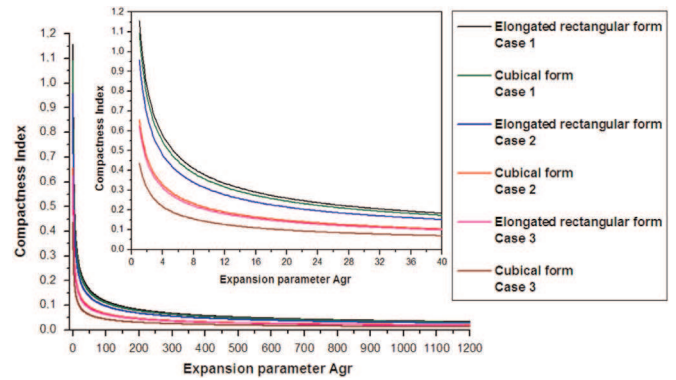


Fig. 13. Variation of the compactness index according to the enlargement order and the geometric shape: the plan enlargement corresponds to multiplying each surface by the  $Agr$  expansion parameter and the internal volume by  $Agr\sqrt{Agr}$ .

1. Room 2 will be transformed into a highly elongated rectangular shape with a dimension of  $V_{room,2}=2(\text{South/North}) \times 16(\text{East/West}) \times 2(\text{height})m^3$ . The corresponding compactness index equal to 0.5625. The internal dimensions of the new plan will be calculated by multiplying each length by 0.5 in the north and south side and by 4 in the east and west side.
2. Room 2 is cubical with side-length  $L (=4$  m), it is the ordinary case of the previously plane; the calculated compactness index is equivalent to 0.5.

To be more realistic in our results, we make an enlargement which corresponds to  $Agr=4$ . Accordingly, the habitable volume will become  $V_{room,2}=2\sqrt{4}(\text{South/North}) \times 16\sqrt{4}(\text{East/West}) \times 2\sqrt{4}(\text{height})m^3$  in the first case, and will become  $V_{room,2}=4\sqrt{4} \times 4\sqrt{4} \times 4\sqrt{4}m^3$  for the second case. The values of the new compactness indices are equal to 0.2813 and 0.25 respectively. Fig. 14 predicts the possible scenarios of the behavior of the simulated temperatures for initial conditions in the vicinity of 31 °C.

These aspects, labeled in Fig. 12, are marked directly on the interior comfort; indoor temperatures undergo an improvement and increasingly approximate to the desired temperature (27 °C). These results justify the improvement of the thermal insulation level, so we proved that the geometry of such construction can provide a direct effect on the buildings thermal performance which can be characterized by the balance between the heat losses and heat gains taking into account their heat storage capacity. The level of thermal insulation can refer to the geometric methods used to reduce heat transfer.

$S$  is the exposed surface to the external environment, including the openings surfaces, therefore this parameter reacted automatically in parallel with compactness. Good compactness is equivalent to a reduction of the deperditive surfaces. During the summer months, to protect against direct solar gain, reducing openings surfaces with double glazing is required, which can slightly penalize natural lighting. However, by reducing glazing surfaces the level of thermal insulation increases and consequently, the heat losses are potentially lower. Reduction in glazing surfaces results in less solar gain and thereafter less heat. In parallel, there is less natural lighting and therefore a slight increase in the consumption for artificial lighting. We understand that to meet the visual comfort, the used energy is dissipated as heat. Otherwise, the smallest opening area reduces the possibility of removing heat by aeration. The major problem of the region is to seek an alternative to improve the thermo-aeraulic comfort, not visual comfort because even if we minimize the vertical surfaces of openings, solar radiation is still intense; this property is entrusted to these climatic regions.

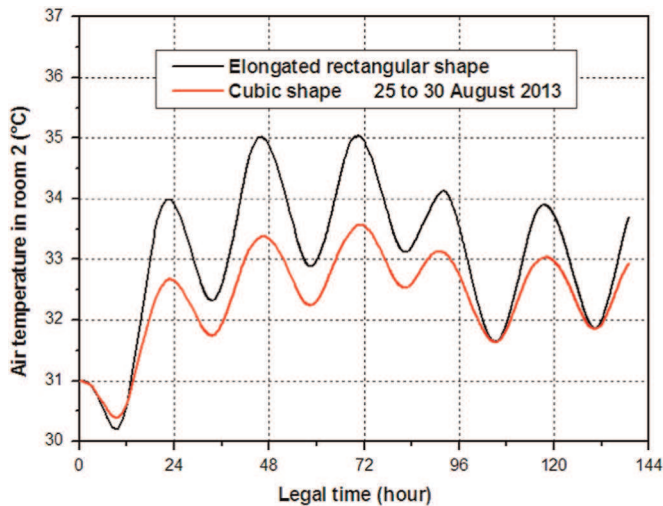


Fig. 14. Simulated temperature of air in room 2.

Solar gains due to the sunlight glazing are the most important; they can represent 50%–80% of total expenses of a conditioned space. The patio home can be an effective solution especially in summer comfort; the patio constitutes a light shaft and favors the natural ventilation. A solution can be also successful if we use eaves or advances roof to create shading without closing the openings.

In winter the problem does not arise, one can enjoy both natural lighting and direct solar gain by letting the blinds open.

## 6. Conclusion

The mechanisms necessary to make low energy buildings exist, are in use, and are legislated for through the evolution of the building regulations. The buildings thermal performance can be characterized by the balance between the heat losses and heat gains taking into account their heat storage capacity. In this balance the three fundamental parameters are the insulation level, thermal inertia use and solar radiation control. In this paper, the results give indications about the importance of compactness. We deduce that consideration of building geometry is useful in evaluating a building's potential for energy use reduction.

Under this Southern climate, the selected days correspond to a very hot period. We conducted this choice because generally 70% of the days of the year are hot (specification of this climate). The results show that shape coefficient is not the only parameter to be considered in the first stage of the design process, solar radiation is the most major contributor to heat gain in buildings. In this Saharan climate, the highest level of daily average solar insolation is received on the horizontal, followed by the south, east/west and north wall. It is essential to reduce the exposed wall surfaces to protect them from overheating in summer. Simulated temperatures prove that the thermal comfort depends on the building materials, thermal inertia and compactness index which characterizes the building size, the geometric shape and the contact mode with the outside. Thermal inertia is responsible for the reduction of inside air temperature peaks and for the delay between the accumulation of energy and its respective release. The design parameters affecting the conservation of energy and factors that affect thermal comfort in the design phase are as follows: location area, number of storeys, building shape, building size, wall height and thermophysical features of the building envelope. Small  $S/V$  ratios imply minimum heat gain and minimum heat loss. For total exposure, to minimize heat transfer through the building envelope

the building shape should be as compact as possible, tending toward a cube. The shape influence tends to disappear with increasing size.

In this warm climate and for a single house, less heat through the windows in summer is positive and negative in winter, less light through the bay windows corresponds to high electricity consumption for lighting. A better compactness induces automatically a higher lighting consumption by comparing it with power consumption due to air conditioning. Despite this constraint, we can always judge that a good compactness brings benefits in terms of thermo-aeraulic comfort but by a slight penalty of the natural lighting and the visual comfort. To overcome this lighting problem, conversely to an individual house, urban scale is the best path to follow, it was agreed to adhere strictly to a compact urban organization with houses that includes patios equipped with openings to ensure better lighting and ventilation. Introversion of homes, through their organizations around a courtyard, greatly reduces the exposed surfaces to the outside; it is a climate and social response.

Like other types of climate, the drawn conclusions and compactness rule remain valid for winter season and even for extreme conditions.

## References

- [1] B.C. Amarilla, Influence of compactness on housing sound insulation costs, *Appl. Acoust.* 35 (1992) 203–219.
- [2] S.M.A. Bekkouche, T. Benouaz, M.K. Cherier, M. Hamdani, M.R. Yaiche, N. Benamrane, Influence of the compactness index to increase the internal temperature of a building in Saharan Climate, *Energy Build.* 66 (2013) 678–687.
- [3] R. Albatichi, F. Passerini, Bioclimatic design of buildings considering heating requirements in Italian climatic conditions, a simplified approach, *Build. Environ.* 46 (2011) 1624–1631.
- [4] P. Depecker, C. Menezio, J. Virgone, S. Lepers, Design of buildings shape and energetic consumption, *Build. Environ.* 36 (2001) 627–635.
- [5] I.Y. Choi, S.H. Cho, J.T. Kim, Energy consumption characteristics of high-rise apartment buildings according to building shape and mixed-use development, *Energy Build.* 46 (2012) 123–131.
- [6] A. Tsanasa, A. Xifarab, Accurate quantitative estimation of energy performance of residential buildings using statistical machine learning tools, *Energy Build.* 49 (2012) 560–567.
- [7] V. Granadeiro, J.R. Correia, V.M.S. Leal, J.P. Duarte, Envelope-related energy demand: a design indicator of energy performance for residential buildings in early design stages, *Energy Build.* 61 (2013) 215–223.
- [8] F. Qi, Y. Wang, A new calculation method for shape coefficient of residential building using Google Earth, *Energy Build.* 76 (2014) 72–80.
- [9] U.T. Aksoy, M. Inalli, Impact of some building passive design parameters on heating demand for a cold region, *Build. Environ.* 41 (2006) 1742–1754.
- [10] S.W. Whang, S. Kim, Determining sustainable design management using passive design elements for a zero emission house during the schematic design, *Energy Build.* 77 (2014) 304–312.
- [11] E. Yasa, V. Ok, Evaluation of the effects of courtyard building shapes on solar heat gains and energy efficiency according to different climatic regions, *Energy Build.* 73 (2014) 192–199.
- [12] E.H. Mathews, P.G. Richards, C. Lombard A, First-order thermal model for building design, *Energy Build.* 21 (1994) 133–145.
- [13] P. Lauret, H. Boyer, C. Riviere, A. Bastide, A genetic algorithm applied to the validation of building thermal models, *Energy Build.* 37 (2005) 858–866.
- [14] M. Sourbron, L. Helsén, Evaluation of adaptive thermal comfort models in moderate climates and their impact on energy use in office buildings, *Energy Build.* 43 (2011) 423–432.
- [15] S. Goyal, P. Barooah, A method for model-reduction of non-linear thermal dynamics of multi-zone buildings, *Energy Build.* 47 (2012) 332–340.
- [16] D.B. Crawley, L.K. Lawrie, F.C. Winkelmann, W.F. Buhl, Y.J. Huang, C. O. Pedersen, R.K. Strand, R.J. Liesen, D.E. Fisher, M.J. Witte, J. Glazer, *EnergyPlus: creating a new generation building energy simulation program*, *Energy Build.* 33 (2001) 443–457.
- [17] S.A. Klein, J.A. Duffie, W.A. Beckman, TRNSYS – a transient simulation program, *ASHRAE Trans.* 82 (1976) 623–633.
- [18] F.C. Winkelmann, B.E. Birsdall, W.F. Buhl, K.L. Ellington, A.E. Erdem, J.J. Hirsch, S. Gates, DOE-2 supplement, version 2.1.E. Technical Report LBL-34947, Lawrence Berkeley National Laboratory, Berkeley, CA, USA, 1993.
- [19] P.O. Fanger, *The Grid: Thermal Comfort Analysis and Applications in Environmental Engineering*, Publishing Company Malabar, 1982.
- [20] J.J. Roux, Comportement thermique des bâtiments, Institut National des Sciences Appliquées, département de génie civil, INSA de Lyon, 2000.

- [21] Y. Jannot, Transferts thermiques. école des mines, Nancy (2012).
- [22] J.P. Nadeau, J.R. Puiggali, Séchage: des processus physiques aux procédés industriels, Tec & Doc-Lavoisier (1995), ISBN 2-7430-0018-X.
- [23] J.B. Saulnier, A. Alexandre, La modélisation thermique par la méthode nodale, ses principes, ses succès et ses limites, Rev. Gén. Therm. 280 (1985) 363–372.
- [24] J.L. Auger, A. Alexandre, J. Martinet, Fonctionnement de capteurs solaires plans en régime variable, Rev. Gén. Therm. 239 (1981) 811–824.
- [25] A.J. Chapman, Heat Transfer, Macmillan, New York, 1984.
- [26] M. Hamdani, S.M.A. Bekkouche, T. Benouaz, M.K. Cherier, A new modelling approach of a multizone building to assess the influence of building orientation in Saharan climate, Therm. Sci. (2014), <http://dx.doi.org/10.2298/TSCI131217026H>.
- [27] M. Hamdani, S.M.A. Bekkouche, T. Benouaz, M.K. Cherier, N. Benamrane et, O. Halloufi., Effect of orientation of buildings with different materials in distribution of temperatures in walls thickness, in: Proceedings of the 13th International Multidisciplinary Scientific GeoConference SGEM 2013, June 16–22, 2013, pp. 91–98, Renewable Energy Sources and Clean Technologies, Albena, Bulgaria, SGEM Scientific Papers DataBase, doi:10.5593/SGEM2013/BD4/S17.012.
- [28] M.K. Cherier, S.M.A. Bekkouche, T. Benouaz, M. Hamdani, N. Benamrane et, O. Halloufi, Studies and choice of local building materials for Improving interior temperatures of a building located in Ghardaïa region, in: Proceedings of the 13th International Multidisciplinary Scientific GeoConference SGEM 2013, June 16–22, 2013, pp. 235–242, Renewable Energy Sources and Clean Technologies, Albena, Bulgaria. SGEM Scientific Papers DataBase doi:10.5593/SGEM2013/BD4/S17.030.
- [29] M. Hamdani, S.M.A. Bekkouche, T. Benouaz, M.K. Cherier, Study and effect of orientation two rooms of buildings located in Ghardaïa, Algeria, Energy Proc. 18 (00986-1) (2012) 636–642. [http://dx.doi.org/10.1016/S1876-6102\(12, Jun.](http://dx.doi.org/10.1016/S1876-6102(12, Jun.)
- [30] S.M.A. Bekkouche, T. Benouaz, M.K. Cherier, M. Hamdani, M.R. Yaiche, N. Benamrane, A. New, modelling approach of a multizone building, influence of the compactness index in hot climate, 16<sup>èmes</sup> Journées Internationales de Thermique JITH 2013, Marrakech Maroc (2013).
- [31] S.M.A. Bekkouche, T. Benouaz, M.K. Cherier, M. Hamdani, M.R. Yaiche, N. Benamrane, Thermo-aeraulic studies of a multizone building & influence of the compactness index, in: Proceedings of Energy Technologies Conference, EN-TECH-'13, Turkey, December 26–28, 2013.
- [32] P. Rumianowski, J. Brau, J.J. Roux, An adapted model for simulation of the inter-action between a wall and the building heating system, in: Proceedings of the Thermal Performance of the Exterior Envelopes of Buildings IV Conference, Orlando, USA, 1989, pp. 224–233.
- [33] L. Mora, Prédiction des performances thermo-aérauliques des bâtiments par association de modèles de différents niveaux de finesse au sein d'un environnement orienté objet (Thèse de Doctorat), Laboratoire d'Etude des Phénomènes de Transfert Appliqués au Bâtiment, UFR Sciences Fondamentales et Sciences pour l'Ingénieur, université de la rochelle, 2003.
- [34] G. Ritoux, Evaluation numérique des facteurs de forme, Rev. Phys. Appl. 17 (1982) 503–515.
- [35] K. Gairaa, Y. Bakelli, An overview of global solar radiation measurements in Ghardaïa area, south Algeria, Int. J. Energy Environ. 2 (2011) 255–260.
- [36] M. Lacombe, D. Bousri, M. Leroy, M. Mezred, WMO field intercomparison of thermometer screens/shields and humidity measuring instruments, World Meteorological Organization, Instruments and Observing Methods, Report No. 106, Ghardaïa, Algeria, November 2008–October 2009.
- [37] M.R. Yaiche, A. Bouhanik, S.M.A. Bekkouche, A. Malek., T. Benouaz, Revised solar maps of Algeria based on sunshine duration, Energy Convers. Manag. 82 (2014) 114–123.
- [38] S.M.A. Bekkouche, T. Benouaz, M.K. Cherier, M. Hamdani, R.M. Yaiche, R. Khanniche, Influence of building orientation on internal temperature in Saharan climates, building located in Ghardaïa region (Algeria), Int. Sci. J. Therm. Sci. 17 (2013) 349–364.
- [39] S.M.A. Bekkouche, T. Benouaz, N. Benamrane, M.K. Cherier, M. Hamdani, Practical installation methods of thermal insulation in a residential building in hot climate, Published in POWERENG2013, in: Proceedings of 4th International Conference on Power Engineering, Energy and Electrical Drives, 13–17 May 2013, Istanbul, Turkey, Page(s): 1050–1059 ISSN: 2155-5516, DOI 10.1109/PowerEng.2013.6635756.
- [40] S.M.A. Bekkouche, T. Benouaz, M.R. Yaiche, M.K. Cherier, M. Hamdani, F. Chellali, Introduction to control of solar gain and internal temperatures by thermal insulation, proper orientation and eaves, Energy Build. 43 (2011) 2414–2421.
- [41] S.M.A. Bekkouche, T. Benouaz, A. Chekneane, A modelling approach of thermal insulation applied to a Saharan building, Therm. Sci. 13 (2009) 233–244.
- [42] A. Yezioro, B. Dong, F. Leite, An applied artificial intelligence approach towards assessing building performance simulation tools, Energy Build. 40 (2008) 612–620.
- [43] S. Hongois, Stockage de chaleur inter-saisonnier par voie thermochimique pour le chauffage solaire de la maison individuelle (thèse de Doctorat), Ecole doctorale Mécanique, Energétique, Génie civil, Acoustique MEGA, Laboratoire d'accueil: Centre de Thermique de Lyon CETHIL à l'Institut National des Sciences Appliquées de Lyon Soutenue le 1<sup>er</sup> avril 2011.